DESIGN, MODELING, AND ANALYSIS OF MULTI-CHANNEL DEMULTIPLEXER / DEMODULATOR *

David D. Lee and K. T. Woo

TRW Electronic Systems Group
One Space Park
Redondo Beach, CA 90278

I. Introduction

Traditionally, satellites have performed the function of a simple repeater. Newer data distribution satellite architectures, however, require demodulation of many frequency division multiplexed uplink channels by a single demultiplexer/demodulator unit, baseband processing and routing of individual voice/data circuits, and remodulation into time division multiplexed (TDM) downlink carriers. The TRW MCDD (Multichannel Demultiplexer/Multirate Demodulator) operates on a 37.4 MHz composite input signal. Individual channel data rates are either 64 Kbps or 2.048 Mbps. The wideband demultiplexer divides the input signal into 1.44 MHz segments containing either a single 2.048 Mbps channel or thirty two 64 Kbps channels. In the latter case, the narrowband demultiplexer further divides the single 1.44 MHz wideband channel into thirty two 45 KHz narrowband channels.

With this approach the time domain FFT channelizer processing capacity is matched well to the bandwidth and number of channels to be demultiplexed. By using a multirate demodulator fewer demodulators are required while achieving greater flexibility. Each demodulator can process a wideband channel or thirty two narrowband channels. Either all wideband channels, a mixture of wideband and narrowband channels, or all narrowband channels can be demodulated. The multirate demodulator approach also has lower nonrecurring costs since only one design and development effort is needed.

TRW has developed a POC (Proof of Concept) model which fully demonstrates the signal processing functions of MCDD. It is capable of processing either three 2.048 Mbps channels or two 2.048 Mbps channels and thirty two 64 Kbps channels. An overview of important MCDD system engineering issues is presented as well as discussion on some of the BOSS (Block Oriented System Simulation) analyses performed for design verification and selection of operational parameters of the POC model. System engineering analysis of the POC model confirmed that the MCDD concepts are not only achievable but also balances the joint goals of minimizing on-board complexity and cost of ground equipments while retaining the flexibility needed to meet a wide range of system requirements.

II. MCDD Concepts and Architecture

1. MCDD Frequency Plan

The TRW MCDD concept embodies a multistage approach to accommodate different channel bandwidths. Each MCDD operates on a digitized 37.4 MHz bandwidth segment. The initial stage provides channelization into thirty two wideband 1.44 MHz channels corresponding to the wideband data rate of 2.048 Mbps. The signal at this point is either demodulated directly or fed to a second channelizer which subdivides the signal into thirty two 45 KHz channels with 64 Kbps narrowband data rate. In the latter case, the output of the second channelizer is fed to a demodulator which is identical to that used for the wideband channel. This single demodulator recovers all of the thirty two 64 Kbps data streams. Thus, only a single demodulator needs to be provided for each 1.44 MHz subsegment of the input spectrum regardless of whether the subsegment contains a single 2.048 Mbps channel or thirty two 64 Kbps channels.

The WB channel data rate and channel spacing are chosen to maximize the composite FDM signal bandwidth efficiency, and the same ratio of maximum bit rate to channel spacing is maintained for the narrowband

* Work performed for NASA Lewis Research Center (under NASA contract NAS3-25866)

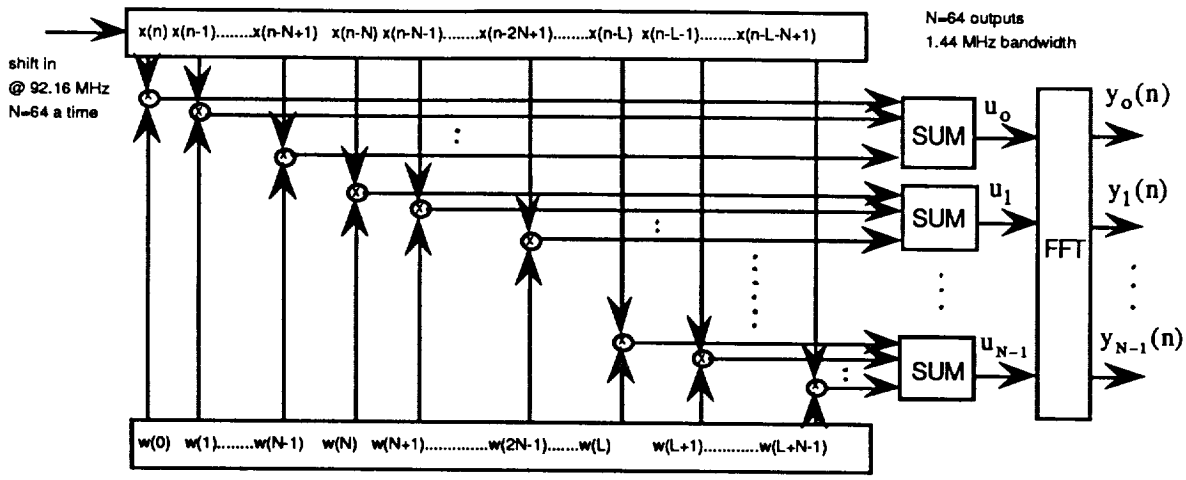

Figure 1. Time Domain FFT Channelizer

channels. Smaller channel spacings place undue frequency and Doppler compensation requirements on the user ground terminals. Larger channel spacings are not only inefficient, but make the typical frequency generation components in the ground terminals unusable. The rate and channel spacing enables a very efficient algorithm to be used within the MCDD for demultiplexing.

2. The Channelizer Design

The TRW MCDD concept uses time domain FFT channelizing in a wideband/narrowband cascade. This algorithm processes the data in the time domain by performing window/presum followed by a single FFT to perform heterodyning of the signal. The FFT channelizer algorithm is important for its efficient use of FFT hardware to realize a parallel bank of filters.

Suppose we require a bank of N complex bandpass filters with equally spaced center frequencies from [DC to f_s), the impulse response of the *k*th filter $h_k(n)$ can be written in terms of a complex modulated lowpass filter w(n)

$$h_k(n) = w(n)e^{-j\left(\frac{2\pi}{N}\right)kn} \quad ; k=0,..N-1 \qquad (1)$$

The Fourier transform shows that the frequency response of the *k*th filter is a frequency shifted version of lowpass filter's frequency response;

$$H_k(e^{j\omega}) = W\left(e^{j\left(\omega+\frac{2\pi}{N}k\right)}\right) \quad ; k=0,...,N-1 \qquad (2)$$

Thus, the *k*th output $y_k(n)$ is given by the convolution

$$y_k(n) = \sum_{m=-\infty}^{\infty} x(n-m)w(m)e^{-j\left(\frac{2\pi}{N}km\right)} \quad ;k=0,...,N-1 \qquad (3)$$

By making substitution : m=Nr+q with q=0,...,N-1 and $-\infty \le r \le \infty$, we can express equation (3) as a double sum

$$y_k(n) = \sum_{q=0}^{N-1}\left[\sum_{r=-\infty}^{\infty} x(n-Nr-q)w(Nr+q)\right]e^{-j\left(\frac{2\pi}{N}kq\right)} \quad ;k=0,...,N-1 \qquad (4)$$

since

$$e^{-j\left(\frac{2\pi}{N}kq\right)} = e^{-j\left(\frac{2\pi}{N}k(Nr+q)\right)}$$

Equation (4) can be rewritten as

$$y_k(n) = \sum_{q=0}^{N-1}[U_n(q)]e^{-j\left(\frac{2\pi}{N}kq\right)} \quad ; k=0,...,N-1 \qquad (5)$$

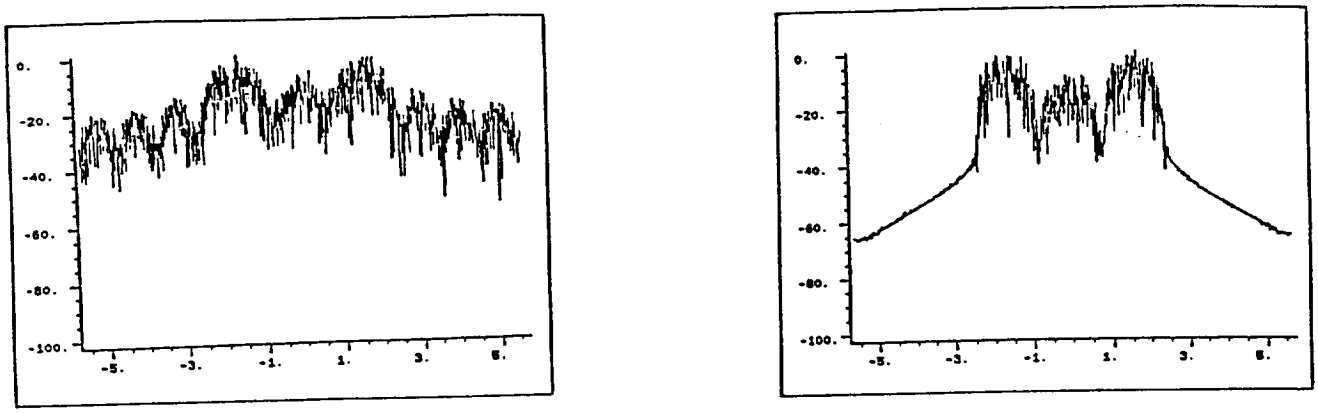

(a) Without Pulse Shaping

(b) With Baseband Pulse Shaping

Figure 2. Power Spectrum of Three Adjacent SQPSK signals when the center channel signal power is 8 dB lower than those of two adjacent channels

where

$$u_n(q) = \sum_{r=-\infty}^{\infty} x(n - Nr - q)w(Nr + q) \quad ; q=0,...,N-1 \qquad (6)$$

Equation (6) is called the presum operation and becomes a finite sum for finite window length. Figure 1 shows a block diagram of the time domain FFT channelizer derived above.

3. Channel Modulation & Pulse Shaping

SQPSK modulation was considered in the initial phase of the MCDD POC development. Figure 2(a) shows the spectra of three adjacent SQPSK signals when the signal of interest (center channel) has 8 dB less signal power than the other two. BER degradation due to such adjacent channel interference (ACI) is quite significant with SQPSK. To mitigate the effects of intersymbol interference (ISI) and the effects of ACI due to bandlimiting in the channelizer, baseband pulse shaping is applied to the SQPSK I and Q symbol pulses. In particular, the pulse shaping function is a raised cosine response with the roll-off factor of 0.3 equally split between the transmitter and the receiver matched filter.

On the other hand, figure 2(b) shows the spectra of the above SQPSK signals with pulse shaping. The effect of ACI is evidently reduced as compared to that of the SQPSK without pulse shaping. This type of baseband pulse shaping, however, will result in a modulated signal which will no longer be constant-envelope. Similar to bandlimiting filtered SQPSK, the transmitter HPA has to be backed off to its linear range in order not to spread the amplified output spectra. Sidelobe level is a function of the amplifier backoff. For an approximately linear mode of operation of a SQPSK transmitter, a 5 dB output backoff would be required, which significantly reduces the transmitter efficiency. To improve the transmitter power efficiency, a constant envelope bandwidth efficient modulation scheme, i.e., Tamed Frequency Modulation, will be required for MCDD in the future. This modulation type can be demodulated with current MCDD architecture. Our 45 KHz narrowband channel spacing matches that of one of the INTELSAT single-channel-per-carrier services which utilize linearly amplified QPSK.

4. The Demodulator Design

Two types of demodulator processing are performed. Narrowband channels are processed by a time domain narrowband FFT channelizer followed by the demodulator, while wideband channels are directly routed to the demodulator bypassing the narrowband channelizer. The narrowband channelizer is conceptually a scaled-down version of the wideband channelizer. After the channelizer separates the FDM signal, it is processed by the multirate demodulator programmed for narrowband operation. A feature of the demodulation is that the same hardware performs both narrowband and wideband functions with a control input determining the operating mode.

The multirate demodulator consists of five major functional blocks: a *resampling filter* to generate exactly two complex signal samples per symbol from the channelizer output of 1.406 samples per symbol and also matched filter the transmitted signal, a *derotate complex multiply* to remove residual carrier phase error from these samples, a *symbol decision* to determine the received two-bit symbol; a *carrier tracking loop* to estimate the carrier

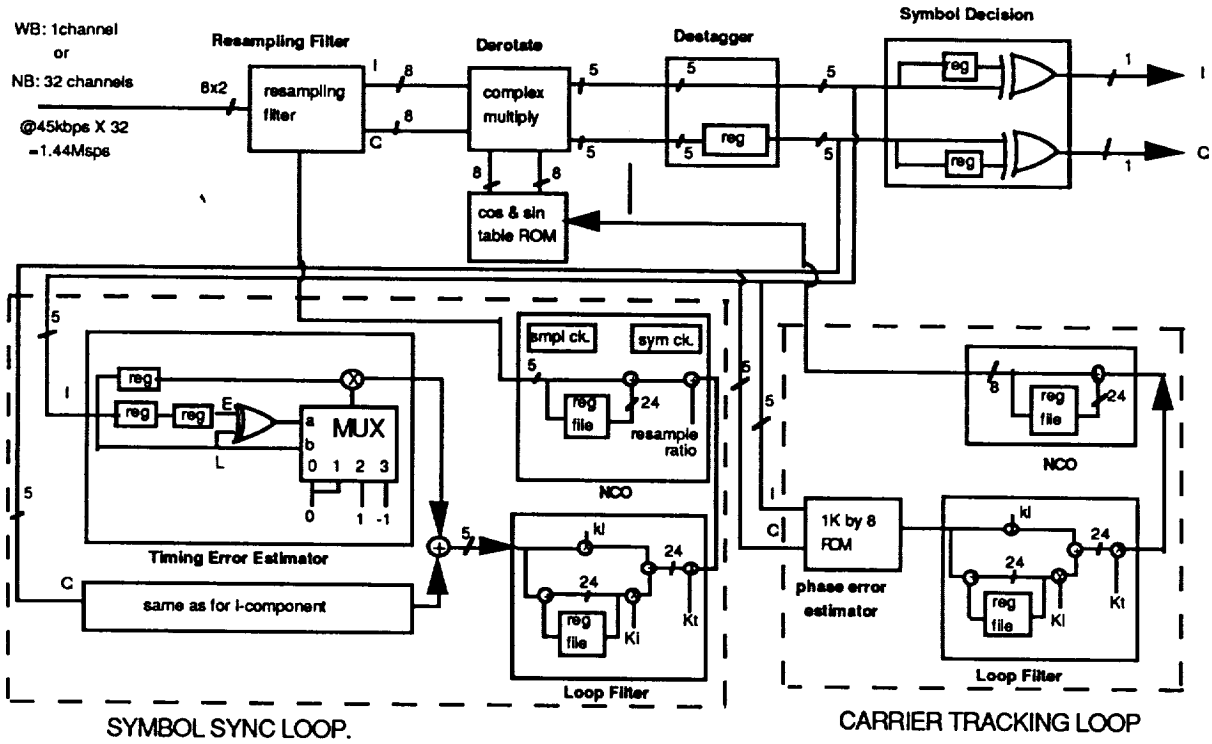

Figure 3. Functional Diagram of the Demodulator

offset to be removed, and a *symbol sync loop* to determine any timing offset to be removed by the resampling filter. Detailed block diagram of the demodulator is shown in Figure 3.

Resampling Filter

The main function of the resampling filter is to resample the data sequence provided by the channelizer at the appropriate sample epochs for the demodulator. The data rate from the channelizer is determined by the ratio of the channel spacing to the symbol rate. Since the narrowband channel spacing is 45 KHz (1.44 MHz for wideband) and the symbol rate is 32 Ksym/sec (2.048 Mbps for wideband), the channelizer output rate is 1.406 samples per symbol. However, the demodulator operation requires 2 samples per symbol for proper timing recovery. Thus the resampler must provide 1.422 samples to the demodulator for every sample provided by the channelizer on the average.

The resampling filter in the MCDD demodulator utilizes the principle of sampling theorem, namely, that a band-limited function is completely determined by its sample values taken at or faster than the Nyquist sampling rate. The reconstructed signal is a summation of appropriately delayed $(\sin x)/x$ functions whose amplitude at the associated sampling instant is exactly the sample value and at every other sampling instant is exactly zero. Furthermore, at all intermediate points in time, the entire collection of terms combines to yield exactly the original continuous waveform everywhere.

In order to do this, the resampling filter works in conjunction with the NCO of the symbol sync loop to interpolate the samples at the correct timing epochs. In order to reduce complexity, the interpolator range is restricted to span only one channelizer sample. Thirty two fractional timing phases are provided by a bank of filter taps. The NCO phase selects the appropriate set for each output sample. Sometimes the resampling filter will compute two output samples for demodulation from a single input sample from the channelizer, and sometimes it will compute only one. (In order for the resampling filter to compute either zero or three samples from a single input sample would require the symbol rate to be off by a degenerate amount.)

Derotator

Because of frequency offsets, Doppler shifts, and phase noise, the complex signal at the output of the channelizer and the resampling filter is not be a true SQPSK baseband signal. That is, the signal at the derotator input is given by

$$\tilde{x}_r(k) = \tilde{x}_b(k)e^{j\theta(k)} \tag{7}$$

where $\tilde{x}_b(k)$ is the true QPSK baseband signal, and $\theta(k)$ is extraneous phase modulation. Because of this extraneous phase modulation, the signal is best described as being a pseudo-baseband signal. The function of the carrier recovery loop is to track the extraneous phase modulation and provide a phase estimate to the derotator for each sample out of the resampling filter. The function of the derotator is to use the phase estimate to translate the pseudo-baseband signal back to the baseband. In order to do this, the derotator multiplies the each input sample by the unit-valued phasor which has a phase in the opposite direction of the phase estimate. The derotator output at time k is thus given by

$$\tilde{x}_d(k) = \tilde{x}_r(k)e^{-j\hat{\theta}(k)} = \tilde{x}_b(k)e^{j(\theta(k)-\hat{\theta}(k))} \tag{8}$$

where $\hat{\theta}$ is the phase estimate provided by the carrier tracking loop at time k, and $\theta(k)-\hat{\theta}(k)$ is the residual phase noise. Appropriate design of the carrier tracking loop produces a residual phase noise process with an acceptable RMS value. The implementation of the derotator in integer arithmetic is straight forward.

Carrier Tracking Loop

The carrier phase error estimate taken after the destagger module is low-pass filtered and used to drive a NCO which tracks the carrier phase offset. For computing the loop parameters as shown in figure 3, the following formulae are used:

$$K_1 = \frac{2\xi\omega_n T}{AK_vK_iT} \tag{9}$$

$$K_i = \frac{(\omega_n T)^2}{AK_vK_iT} \tag{10}$$

where A is the carrier phase estimator module gain, K_v is the NCO gain, T is the symbol period, ξ is the damping factor (ξ=0.707), w_n is the loop resonance frequency given by

$$\omega_n = 1.89B_L, \tag{11}$$

and B_L is the desired loop bandwidth.

With loop bandwidth selection of 10^{-2} times the symbol rate ($B_LT=10^{-2}$), the carrier loop will be able to acquire frequency offsets of 102.4 KHz for the wideband channel, and 3.2 KHz for the narrowband channel, both assuming K-band (14 GHz) uplinks. This implies oscillator instabilities of approximately 7.3×10^{-6} and 2.3×10^{-7} for the wideband and narrowband transmitters, respectively. Thus for wideband channels, it is not necessary to provide any special acquisition mechanism, but an acquisition aid may be required for narrowband channels.

Narrower loop bandwidth decreases RMS jitter due to thermal noise, however, this results in slow pull-in time and poorer phase noise performance due to oscillator instability. On the other hand, setting the loop bandwidth too large would allow too much RMS jitter due to thermal noise which results in substantial BER performance degradation. The loop bandwidth in the MCDD POC model is selected to be one hundredth of the data rate which results in phase jitter due to thermal noise less than six degrees and pull in time of less than 0.05 second.

Symbol Synchronization Loop

The derotated complex samples are processed, I and Q separately, to determine timing error. If the two mid-symbol samples are of opposite signs, they will cancel and the transition sample will be near zero. The value of transition sample is therefore zero if the resampling filter is precisely locked to the symbols, and any timing error will be proportional to the non-zero sample value at the transition. The difference in sign of the two mid-symbol

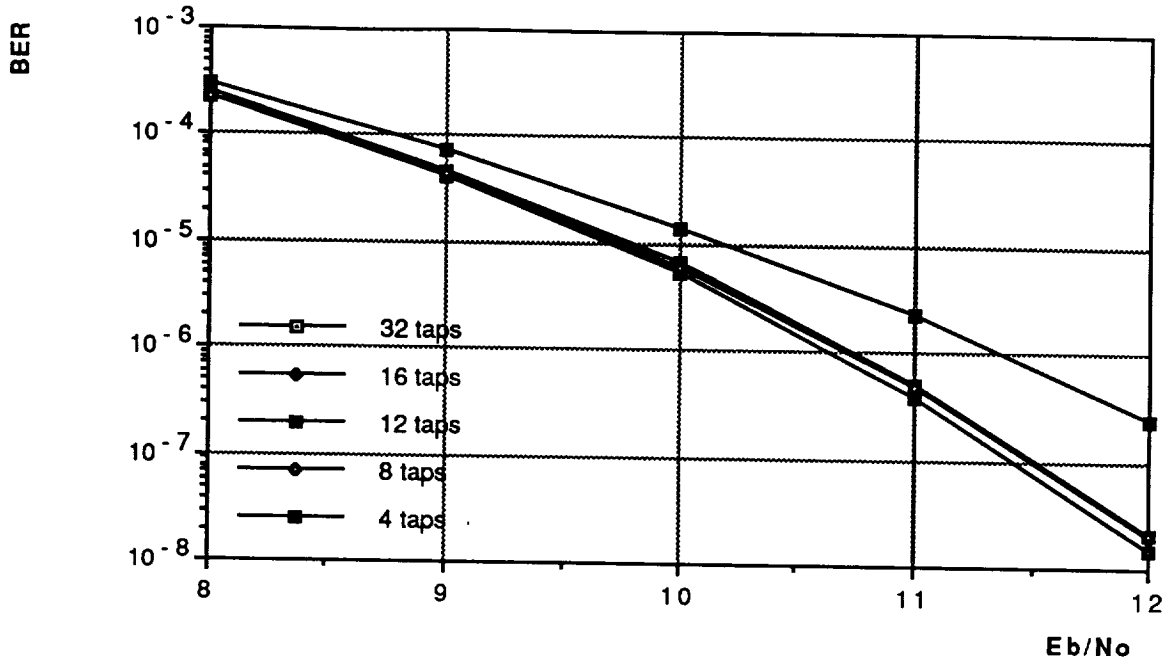

Figure 4. BER vs. No. of Resampling Filter Taps

samples indicates the direction of timing error. If the signs are equal, the above sum is ignored since no transition occurred. The measured timing errors for the I and Q samples are summed to give the resulting timing error estimate.

The timing error estimate is low-pass filtered and used to fine tune the NCO which tracks the timing phase and selects the resampling filter taps. The step size is a function of the fixed ratio of the resampling filter input and output sample rates. The fine tuning tracks variable timing drift. The timing offset is output to the resampling filter to select the next filter to be used. The number of resampling filter taps is chosen to provide good interpolation precision while minimizing the size of the hardware. The loop parameters can be obtained using the equations (9) to (11) as well. With the loop bandwidth selection of 5×10^{-3} times the symbol rate, the bit synchronization loop will be able to acquire clock rate offsets of 51.2 Kbps for the wideband channel, and 1.6 Kbps for the narrowband channel. This implies symbol clock instabilities of 2.5×10^{-2} for both the wideband and narrowband transmitters, thus it is not necessary to provide any special acquisition mechanism in either the wideband or the narrowband case.

III. MCDD Performance Analysis Using BOSS

The Block Oriented Systems Simulator (BOSS) run under VMS operating system on a DEC VAX station provides a complete iterative environment for simulation-based analysis and design of any system signal processing operation. Whereas BOSS can perform a time domain (waveform level) simulation of any system, the current model library contains functional blocks most suitable for communication systems simulation. Performance of the total MCDD as well as each of the individual blocks have been carefully analyzed using BOSS. Furthermore, the BOSS semi-analytic BER estimator module was used to perform the parameter trade study. Shown below are two of the most significant parameter trades performed using BOSS.

The demodulator losses due to resampling filter, carrier tracking loop, bit synchronization loop, and quantization, all in terms of the Eb/No degradation from theory for achieving 5×10^{-7} BER, have been quantified. It was found that most of the performance losses came from the resampling filter. Among many resampling filter parameters, the number of resampling filter taps was found to be the most critical to BER performance. Figure 4 shows the BER plots (with ideal channelizer) *vs.* the number of resampling filter taps. Even though eight seems to be a point of diminishing return, our choice for the number of resampling filter taps is sixteen in order to allow room for implementation losses, and future constant envelope modulation choices, i.e., Tamed Frequency Modulation, which will require the longer filter span.

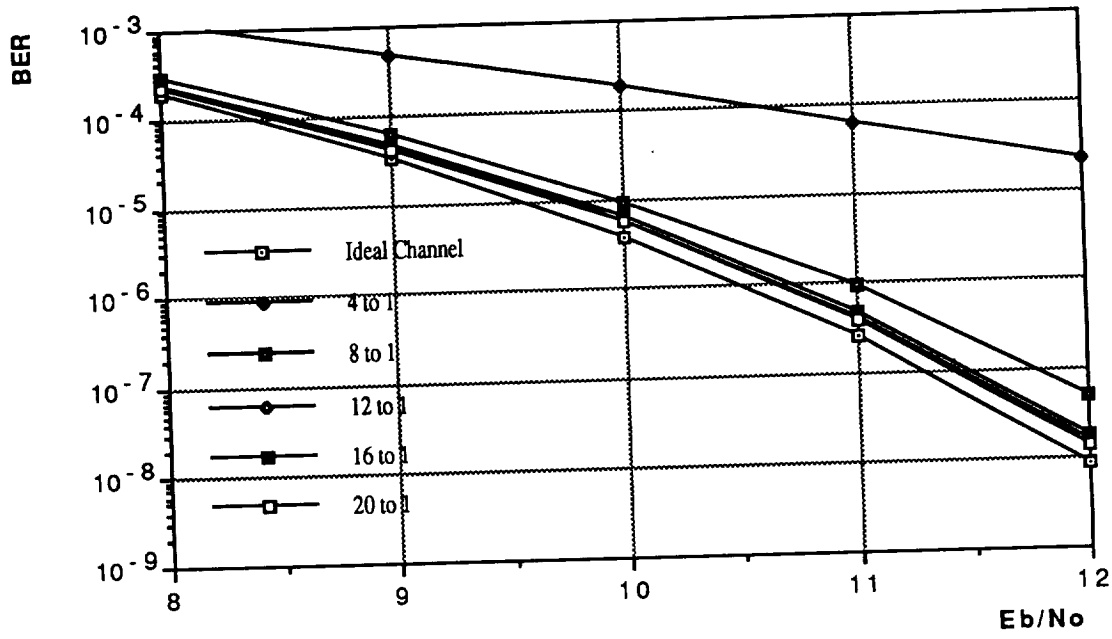

Figure 5. Total BER vs. Channelizer Presum Ratio

The channelizer performance principally depends on the window type and presum ratio. Kaiser window has been chosen for its flat pass-band response at the expense of moderate stopband ripple since the current modulation choice with baseband pulse shaping have already mitigated the effects of ACI. The BER performance improves with increasing presum ratio due to wider 3 dB bandwidth and steeper cutoff. It reaches to the point of diminishing return at around twelve. (see figure 5.) Our choice of the presum ratio is sixteen, however, to allow room for additional implementation losses as well as the possibility of implementing a constant envelope bandwidth efficient type modulation later. In the same manner, we have also chosen the window tap quantization to be sixteen bits after observing significant degradation of BER performance with less than twelve bits.

Raised cosine pulse shaping effectively mitigates the effects of ACI and ISI. The worst case ACI example shown in figure 2(b) only increases the BER by less than one percent over the case without ACI. Total MCDD BER estimates have been obtained using the chosen parameters and linearly amplified SQPSK modulation. Note the 0.25 dB Eb/No degradation at the BER of 5×10^{-7} with the presum ratio of 16 to 1 (see figure 5). This compares with about 0.1 dB Eb/No degradation due to the demodulator alone.

IV. Conclusions

A overview of important MCDD system engineering issues have been presented as well as discussion on some of the BOSS analyses performed for design verification and selection of operational parameters of the POC model. The bandwidth-efficient FDM composite signal structure, linearly amplified SQPSK modulation, and time domain FFT channelization method were chosen based on the TRW's space communication system engineering experience and trade studies. Virtually no constraints are imposed by this FDM composite signal structure, which is feasibly implementable on-board due to the efficient wideband and narrowband channelization cascade. The coherent SQPSK demodulator, implementable on-board in advanced VLSI, offers robust operation with imperfect user synchronization.

Acknowledgments

Much of the demodulator design and simulation analysis is due to Mr. G. Caso of the SEIT Organization. The authors also would like to thank Mr. M. Spencer of the Digital Design Laboratory for providing theoretical basis and a preliminary hardware design for the FFT channelizer .